Novel homozygous *ENPP1* mutation causes generalized arterial calcifications of infancy, thrombocytopenia, and cardiovascular and central nervous system syndrome

Orna Staretz-Chacham[1,2], **Rachel Shukrun**[3,4], **Ortal Barel**[5], **Ben Pode-Shakked**[4,6,7], **Oren Pleniceanu**[3,4], **Yair Anikster**[4,6], **Nechama Shalva**[6], **Carlos R. Ferreira**[8], **Admit Ben-Haim Kadosh**[2], **Justin Richardson**[2], **Shrikant M. Mane**[9], **Friedhelm Hildebrandt**[10], **Asaf Vivante**[3,4,7,10]

[1]Metabolic Clinic, Pediatric Division, Soroka Medical Center, Ben-Gurion University, Be'er Sheva, Israel [2]Department of Neonatology, Soroka University Medical Center, Faculty of Health Sciences, School of Medicine, Ben-Gurion University of the Negev, Be'er Sheva, Israel [3]Edmond and Lily Safra Children's Hospital, Sheba Medical Center, Ramat-Gan, Israel [4]Sackler School of Medicine, Tel Aviv University, Tel Aviv, Israel [5]The Genomic Unit, Sheba Cancer Research Center, Sheba Medical Center, Tel Hashomer, Israel [6]Metabolic Disease Unit, Edmond and Lily Safra Children's Hospital, Sheba Medical Center, Ramat-Gan, Israel [7]Talpiot Medical Leadership Program, Department of Pediatrics B and Pediatric Nephrology Unit, Sheba Medical Center, Ramat-Gan, Israel [8]Medical Genetics Branch, National Human Genome Research Institute, National Institutes of Health, Bethesda, Maryland [9]Department of Genetics, Yale University School of Medicine, New Haven, Connecticut [10]Department of Medicine, Boston Children's Hospital, Harvard Medical School, Boston, Massachusetts

Abstract

Generalized arterial calcifications of infancy (GACI) is caused by mutations in *ENPP1*. Other *ENPP1*-related phenotypes include pseudoxanthoma elasticum, hypophosphatemic rickets, and Cole disease. We studied four children from two Bedouin consanguineous families who presented with severe clinical phenotype including thrombocytopenia, hypoglycemia, hepatic, and neurologic manifestations. Initial working diagnosis included congenital infection; however, patients remained without a definitive diagnosis despite extensive workup. Consequently, we investigated a potential genetic etiology. Whole exome sequencing (WES) was performed for affected children and their parents. Following the identification of a novel mutation in the *ENPP1* gene, we characterized this novel multisystemic presentation and revised relevant imaging studies. Using WES, we identified a novel homozygous mutation (c.556G > C; p.Gly186Arg) in *ENPP1* which affects a highly conserved protein domain (somatomedin B2). *ENPP1*-associated genetic diseases exhibit phenotypic heterogeneity depending on mutation type and location. Follow-up clinical characterization of these families allowed us to revise and detect new features of systemic

Correspondence: Asaf Vivante, Talpiot Medical Leadership Program, Pediatric Department B and Pediatric Nephrology Unit, Chaim Sheba Medical Center, Tel Aviv, Israel. asaf.vivante@sheba.health.gov.il or asafvivante@gmail.com.

calcifications, which established the diagnosis of GACI, expanding the phenotypic spectrum associated with *ENPP1* mutations. Our findings demonstrate that this novel *ENPP1* founder mutation can cause a fatal multisystemic phenotype, mimicking severe congenital infection. This also represents the first reported mutation affecting the SMB2 domain, associated with GACI.

Keywords

ENPP1; generalized arterial calcifications of infancy; WES

1 | INTRODUCTION

ENPP1 is a member of the ectonucleotide pyrophosphatase/phosphodiesterase (ENPP1) family. The encoded protein is a Type II transmembrane glycoprotein that has broad specificity and cleaves a wide range of substrates. *ENPP1*-associated genetic diseases exhibit phenotypic heterogeneity depending on mutation type and location (Eytan et al., 2013; Nitschke et al., 2012; Rutsch et al., 2003). Biallelic mutations in this gene cause generalized arterial calcifications of infancy (GACI) [OMIM#208000] (Rutsch et al., 2003), pseudoxanthoma elasticum (Nitschke et al., 2012), and hypophosphatemic rickets [OMIM# 613312] (Levy-Litan et al., 2010; Lorenz-Depiereux, Schnabel, Tiosano, Hausler, & Strom, 2010). Biallelic or heterozygous mutations affecting its dimerization cause Cole disease [OMIM# 615522], a rare dermatologic disease featuring keratoderma and patchy hypopigmentation lesions (Eytan et al., 2013). In addition, risk variants in *ENPP1* have been reported to be associated with childhood obesity and glucose intolerance (Meyre et al., 2005).

GACI is a rare fatal disease that presents in early infancy. The disease is characterized by early onset widespread calcifications along the internal elastic lamina of medium- and large-sized arteries with narrowing of the vessels, resulting in severe hypertension, respiratory distress, and heart failure. Many cases are diagnosed at autopsy (Bird, 1974). Involvement of the coronary arteries leads to early death, with most patients dying within the first 6 months of life (Ciana et al., 2006; Meradji, de Villeneuve, Huber, de Bruijn, & Pearse, 1978).

As noted above, the majority of cases arise from biallelic loss of function mutations in the *ENPP1* gene that encodes an ENPP1, a cell surface protein that breaks-down ATP to AMP and inorganic pyrophosphate (PPi). Thus, these mutations result in decreased synthesis of PPi, causing a low PPi/Pi ratio, leading to ectopic calcium depositions due to lack of PPi inhibition (Eller et al., 2008; Li, van de Wetering, & Uitto, 2019; Nitschke & Rutsch, 2012).

Here, we report an unusual and severe phenotypic presentation of GACI, caused by a novel founder *ENPP1* mutation, in individuals from two Bedouin consanguineous pedigrees. Affected patients presented in the neonatal period with a fatal multiorgan syndrome characterized by thrombocytopenia, hypoglycemia, hepatic, central nervous system (CNS), and respiratory abnormalities. Clinical manifestations were suggestive of a congenital infection but eventually, following an extensive laboratory evaluation, no laboratory evidence for congenital infection could be found. Death ensued within the first 6 months of

life. We found that the novel *ENPP1* founder mutation segregated with this severe multisystemic presentation.

2 | METHODS

2.1 | Study participants

After informed consent, we obtained clinical data, blood samples, and pedigrees from individuals participating in this study. Approval for research on humans was obtained from the Boston Children's Hospital and Sheba Medical Center Review Boards. The clinical diagnosis of the multisystemic syndrome was made by a pediatric neonatologist.

2.2 | Whole exome sequencing

Whole exome sequencing (WES) was performed using genomic DNA isolated from blood lymphocytes and later processed using Agilent SureSelect human exome capture kits (Life Technologies) with next-generation sequencing on an Illumina sequencing platform at the Broad Institute (Cambridge, MA) and Yale Center for Mendelian Genomics (New Haven, CT). Sequence reads were mapped to the human reference genome assembly (NCBI build 37/hg19; www.genome.ucsc.edu) using CLC Genomics Workbench (version 6.5.1) software (CLC Bio, Aarhus, Denmark), as previously described (Vivante et al., 2017).

2.3 | Variant calling

Following WES, genetic variants were first filtered to retain only non-synonymous changes. Second, filtering was performed to retain only alleles with a minor allele frequency (MAF) of <0.01. MAF was estimated using combined datasets incorporating all available data from the 1,000 Genomes Project, the Exome Variant Server project, dbSNP142, and the Genome Aggregation Database (gnomAD). Third, observed sequence variants were analyzed using the UCSC Human Genome Bioinformatics Browser for the presence of paralogous genes, pseudogenes, or misalignments. Fourth, we scrutinized all variants within the sequence alignments of the CLC Genomic Workbench software program for poor sequence quality and for the presence of mismatches that indicate potential false alignments. Fifth, we employed web-based programs to assess variants for evolutionary conservation, to predict the impact of disease candidate variants on the encoded protein, and to determine whether these variants represented known disease-causing mutations. Mutation calling was performed by a team of clinician scientists, who had knowledge of the clinical phenotypes and pedigree structure, as well as experience with homozygosity mapping and exome evaluation as previously described (Vivante et al., 2017). Sanger sequencing was performed to confirm the remaining variants in original DNA samples and when available to test for familial segregation of phenotype with genotype.

2.4 | Sanger sequence analysis of ENPP1

Primers were designed to amplify exon 4 of the *ENNP1* gene. Genomic DNA was amplified by polymerase chain reaction (PCR) using the primers F: 5′TTACCCCATTAGTTCAGAGTGGCC3′; R:5′TGAGACACATTA AGA CAGATTCCAAAAAC3′ (Red Load Taq master mix, Larova GmbH, Teltow, Germany). PCR products were analyzed by nucleotide sequencing using Big Dye Termination

chemistry and an ABI Prism 3100 sequencer (V1.1, Applied Biosystems, Foster City, CA). Sequence analysis was performed using Bioedit software, and sequence chromatograms were visually analyzed for mutation.

3 | RESULTS

3.1 | Clinical findings

We identified four children from two consanguineous families (Figure 1a) who presented with multisystemic manifestations (Table 1 and Table S1).

3.2 | Family A

Patient A-I was the first son of consanguineous Bedouin parents. Polyhydramnios was detected during pregnancy, and the patient was born prematurely at 33 weeks' gestational age. Birth weight was 1,820 g (50th percentile) and head circumference 30 cm (50th percentile). The patient presented with respiratory distress syndrome that was treated with noninvasive respiratory support and resolved after 3 days. After birth, he developed persistent hypoglycemia with high insulin levels, accompanied by polycythemia that did not resolve after dilution, and thrombocytopenia that improved during hospitalization without treatment. Moreover, the patient developed cholestasis at the age 10 days with acholic stools. The initial work-up, which included blood gases, ammonia, lactate, acylcarnitine profile, urine reducing substances, and muscle biopsy, was normal. Urine organic acid analysis showed a mild increase in tyrosine metabolites without elevation of succinylacetone. The patient was readmitted at the age of 2 months due to systemic shock necessitating massive resuscitation with elevated liver enzymes, lactic acidosis, and thrombocytopenia. Echocardiography showed significant septal hypertrophy, mitral regurgitation, tricuspid regurgitation, and decreased contractility. Brain magnetic resonance imaging (MRI) revealed old strokes, marked gliotic changes, and bilateral occipital necrosis (Figure 2a). Liver biopsy demonstrated canalicular cholestasis. His condition deteriorated and he succumbed after a few days.

Patient A-II was the second child in Family A (female). Polyhydramnios was detected during pregnancy, and the patient was born prematurely at 33 + 5 weeks' gestational age via emergency cesarean section due to breech presentation with premature contractions. Birth weight was 2,452 g (50th percentile) and head circumference 31 cm (50th percentile). Similar to her brother, she developed respiratory distress syndrome treated with invasive ventilation and high oxygen requirement until her death. The patient was born with severe thrombocytopenia. Physical examination revealed mild dysmorphic features, encephalopathy with low muscle tone, and absent reflexes. Her abdomen was distended and she was noted to have petechial rash and severe pitting edema. Work-up included blood cultures, TORCH, and enterovirus serology, which were all negative. Head sonogram showed a left choroid plexus cyst with bilateral ventriculomegaly and periventricular calcifications. Echocardiography demonstrated patent foramen ovale, patent ductus arteriosus, mild mitral regurgitation, aortic calcifications, and hypertrophy with pericardial effusion (Figure 2b). Abdominal sonogram showed mild hepatomegaly and ascites. The patient was treated with

antibiotics, fresh frozen plasma, and repeated platelet infusions, but her condition deteriorated and she died at 3 days.

Patient A-III was the third child in Family A (male). This pregnancy was also notable for polyhydramnios and the patient was born premature, at 31 weeks' gestational age. Birth weight was 1,530 g (50th percentile) and head circumference 28 cm (50th percentile). Following birth, the patient had respiratory distress syndrome that was treated with invasive ventilation and high oxygen requirement until his death. Physical examination demonstrated mild dysmorphic features, encephalopathy with increased muscle tone, and distended abdomen. The patient did not pass stool, with no other evidence for bowel obstruction, and succumbed at the age of 11 days. Work-up included blood cultures, Chromosomal microarray analysis, and GM1 gangliosidosis test, which were all negative. Blood tests revealed elevated gamma-glutamyl transpeptidase levels as well as repeated elevations of lactate. Head sonogram showed mild ventriculomegaly with lenticulostriate vasculopathy. Echocardiography revealed decreased contractility and hyperechogenicity of large blood vessels. Revision of imaging studies revealed significant arterial calcifications demonstrated in prenatal sonogram as well as in chest X-ray performed several days postdelivery (Figure 2c,d).

3.3 | Family B

Patient B-I was the first son of consanguineous Bedouin parents. During pregnancy, the mother presented with polyhydramnios and the patient was born prematurely at 36 + 2 weeks' gestational age with meconium-stained amniotic fluid. The patient was born small for gestational age, birth weight was 1,745 g and head circumference 31 cm (<3rd percentile). At birth, he developed severe hypoglycemia that necessitated a D10 continuous infusion, as well as severe thrombocytopenia that required repeated platelet infusions and did not respond to immunoglobulins. On Day 4, the patient developed systemic hypertension treated with hydralazine. Subsequent laboratory work-up was unremarkable except for elevated renin and aldosterone (Table S1).

Renal Doppler ultrasonography demonstrated renal artery stenosis with more than 60% obstruction of the left renal artery and a very small right kidney. Brain ultrasonography revealed bilateral ventriculomegaly (Figure 2e), followed by brain MRI that demonstrated signs of global brain ischemia and cystic periventricular leukomalacia. Due to significant hydrocephalus, insertion of a ventriculoperitoneal shunt was required. Echocardiography demonstrated hypertrophy of the left chamber secondary to systemic hypertension. Abdominal computed tomography scan revealed significant aortic and iliac arteries calcifications (Figure 2f). The patient was started on bisphosphonates at 1 month of age; however, his disease progressed and he died at 6 months.

3.4 | Genetic analysis identifies a novel ENPP1 mutation

Given the lack of a definitive diagnosis in these families, we performed WES analysis in all affected individuals and their parents. We identified a novel *ENPP1* mutation (NM_006208.3: c.556G>C; p.Gly186Arg) located in the last nucleotide of exon four. This mutation is predicted to be deleterious (SIFT, Polyphen2—HDIV [HumDiv; 0.999],

Polyphen2—HVAR [HumVar; 0.986], MutationTaster [disease causing], and CADD score of 34) by affecting a highly conserved protein domain (somatomedin B2 domain; Figure 1b). Interestingly, this novel variant is exceedingly rare and was not found in over 130,000 individuals in gnomAD nor in our inhouse cohort of 2,056 Israeli exomes.

Given the multisystemic nature of the disease, *ENPP1*-related monogenic disease was not initially suspected on clinical grounds in either family before the return of genetic results. Follow-up clinical characterization of the patients allowed us to revise and detect relevant new clinical features in a more appropriate pathogenetic context. This included systemic calcifications noted on review of all patients' imaging studies (Figure 2), thereby establishing the diagnosis of GACI.

3.5 | Delineation of the consequences of c.556G>C mutation

In order to further investigate the consequences of the novel ENPP1 mutation, we performed a splice site bioinformatics analysis using the Berkeley Drosophila Genome Project splice site prediction tool (http://www.fruitfly.org/seq_tools/splice.html). The analysis revealed that this change is predicted to result in a deletion of the 5′ splice site (donor splicing site) at the end of exon 4. As a result, exon 4 is predicted to be longer, coding for the synthesis of 48 additional amino acids until a stop codon prematurely appears.

Next, we extracted RNA from fibroblast cell cultures established from a skin biopsy obtained from a carrier of the novel *ENPP1* mutation (father in Family A). cDNA was synthesized, and the mutation carrier exhibited only the wild-type *ENPP1* mRNA isoforms (Figure S1). We hypothesized that this may indicate that the predicated mutated mRNA segment was most probably degraded via nonsense-mediated decay mechanism that reduces errors in gene expression by eliminating mRNA transcripts that contain premature stop codons.

4 | DISCUSSION

We report herein four cases from two Bedouin consanguineous families harboring a novel *ENPP1* founder mutation. All patients presented at birth with a severe multisystemic disease leading to early death within the first 6 months of life. All patients had significant CNS abnormalities (Table 1), which included periventricular calcifications (Patient A-II) and lenticulostriate vasculopathy (Patient A-III). These findings, in addition to severe thrombocytopenia and mild liver dysfunction, noted in three out of the four affected individuals, initially triggered a common working diagnosis of congenital infection (e.g., TORCH). Eventually, no laboratory evidence for congenital infection could be found and patients succumbed without a diagnosis, which led us to perform genetic analysis. The *ENPP1* mutation revealed by WES in our patients was not suspected on clinical grounds before this study. Review of the patients' imaging studies following the establishment of the molecular genetic diagnosis led to an unequivocal etiology-based diagnosis of GACI, thus expanding the known phenotypic spectrum associated with *ENPP1* mutations.

Early diagnosis of GACI by prenatal ultrasound detection of vascular calcifications can have a crucial clinical importance. If detected early, therapeutic interventions could be initiated at

the time of diagnosis. Treatment approaches including administration of bisphosphonates, magnesium supplementation, and recombinant ENPP1 enzyme replacement therapy have been shown to be beneficial in animal models of GACI (Albright et al., 2015; Huesa, Staines, Millan, & MacRae, 2015; Kingman, Uitto, & Li, 2017; Li, Kingman, Sundberg, Levine, & Uitto, 2016). Some prominent clinicians advocate the maternal administration of bisphosphonates and postnatal treatment of sodium thiosulfate (https://www.chop.edu/ giving/stories/generalized-arterialcalcificationinfancy-gaci-natalies-story). Novel therapeutic options emphasize the importance of an early diagnosis.

GACI is a severe fatal disease with an estimated frequency of 1:390,000 (GeneReview). The first description in the English language medical literature of a patient with a clinical picture of GACI was in 1901 (GeneReview). The most common disease characteristics are arterial hypertension, respiratory distress, cyanosis, and failure to thrive. Approximately 200 cases have been reported worldwide (Amine et al., 2015). Loss of function mutations in the *ENPP1* gene have been found in 69–80% of cases (Nael, Siaghani, Chen, Romansky, & Shane, 2014; Nitschke & Rutsch, 2012; Rutsch et al., 2008; Rutsch, Nitschke, & Terkeltaub, 2011). The underlying pathogenesis of the disease is severe calcification of the internal elastic lamina in large- and medium-sized arteries, as well as proliferation of the intima leading to arterial stenosis. The disease is known to affect multiple systems, and therefore would be expected to involve additional organs such as the brain. Thus far, CNS involvement is reported in several cases (Glatz, Pawel, Hsu, Weinberg, & Chrisant, 2006; van der Sluis, Boot, Vernooij, Meradji, & Kroon, 2006), presenting strokes (Van Dyck, Proesmans, Van Hollebeke, Marchal, & Moerman, 1989), recurrent transient ischemic attacks due to cerebrovascular insufficiency (Thomas et al., 1990), or seizures (Prior & Bergstrom, 1948), (Galletti et al., 2011). In addition, cystic encephalomalacia was reported in one individual with mutation of *ENPP1* (Galletti et al., 2011).

ENPP1 consists of eight domains (Figure 1b; Jansen et al., 2012). *ENPP1*-associated genetic diseases exhibit phenotypic heterogeneity depending on mutation type and location. Biallelic mutations with recessive inheritance cause GACI and hypophosphatemic rickets. Most mutations associated with ectopic calcification affect the phosphodiesterase domain, which is thought to mediate ENPP1 catalytic activity, or the nuclease domain. Biallelic or heterozygous *ENPP1* mutations, thus with either dominant or recessive inheritance, were reported to cause Cole disease, a rare genodermatosis featuring punctate keratoderma, patchy hypopigmentation, and cutaneous calcifications (Chourabi et al., 2018). All reported *ENPP1* mutations leading to Cole disease affect cysteine residues in the somatomedin-B-like domains (SMB1 or SMB2), thus interfering with ENPP1 homodimerization by impairing formation of disulfide bridges. Interestingly, the biallelic homozygous *ENPP1* mutation that we detected affects the SMB2 domain, where no previous GACI-causing mutations had been described to date. We hypothesize that this may explain the nontypical clinical presentation of the affected individuals harboring this mutation.

In summary, we describe a novel *ENPP1* founder mutation associated with a fatal multisystemic disease mimicking severe congenital infection. This represents the first reported mutation in the SMB2 domain associated with arterial calcification. Our data also expand the phenotypic spectrum of *ENPP1*-releated phenotypes.

Supplementary Material

Refer to Web version on PubMed Central for supplementary material.

REFERENCES

Albright RA, Stabach P, Cao W, Kavanagh D, Mullen I, Braddock AA, … Braddock DT (2015). ENPP1-Fc prevents mortality and vascular calcifications in rodent model of generalized arterial calcification of infancy. Nature Communications, 6, 10006 10.1038/ncomms10006

Amine M, Faten H, Rim H, Nidhal HS, Njim L, Moussa A, & Zakhama A (2015). A rare cause of death in infancy: Idiopathic infantile arterial calcification. Pathologica, 107(1), 29–31. [PubMed: 26591630]

Bird T (1974). Idiopathic arterial calcification in infancy. Archives of Disease in Childhood, 49(2), 82–89. [PubMed: 4274089]

Chourabi M, Liew MS, Lim S, H'Mida-Ben Brahim D, Boussofara L, Dai L, … Reversade B (2018). ENPP1 mutation causes recessive Cole disease by altering melanogenesis. The Journal of Investigative Dermatology, 138(2), 291–300. 10.1016/j.jid.2017.08.045 [PubMed: 28964717]

Ciana G, Trappan A, Bembi B, Benettoni A, Maso G, Zennaro F, … Rutsch F (2006). Generalized arterial calcification of infancy: Two siblings with prolonged survival. European Journal of Pediatrics, 165(4), 258–263. 10.1007/s00431-005-0035-6 [PubMed: 16315058]

Eller P, Hochegger K, Feuchtner GM, Zitt E, Tancevski I, Ritsch A, … Mayer G (2008). Impact of ENPP1 genotype on arterial calcification in patients with end-stage renal failure. Nephrology, Dialysis, Transplantation, 23(1), 321–327. 10.1093/ndt/gfm566

Eytan O, Morice-Picard F, Sarig O, Ezzedine K, Isakov O, Li Q, … Sprecher E (2013). Cole disease results from mutations in ENPP1. American Journal of Human Genetics, 93(4), 752–757. 10.1016/j.ajhg.2013.08.007 [PubMed: 24075184]

Galletti S, Nitschke Y, Malavolti AM, Aquilano G, Faldella G, Corvaglia L, & Rutsch F (2011). Generalized arterial calcification of infancy: Fatal clinical course associated with a novel mutation in ENPP1. JIMD Report, 1, 23–27. 10.1007/8904_2011_11

Glatz AC, Pawel BR, Hsu DT, Weinberg P, & Chrisant MR (2006). Idiopathic infantile arterial calcification: Two case reports, a review of the literature and a role for cardiac transplantation. Pediatric Transplantation, 10(2), 225–233. 10.1111/j.1399-3046.2005.00414.x [PubMed: 16573612]

Huesa C, Staines KA, Millan JL, & MacRae VE (2015). Effects of etidronate on the Enpp1(−)/(−) mouse model of generalized arterial calcification of infancy. International Journal of Molecular Medicine, 36(1), 159–165. 10.3892/ijmm.2015.2212 [PubMed: 25975272]

Jansen S, Perrakis A, Ulens C, Winkler C, Andries M, Joosten RP, … Bollen M (2012). Structure of NPP1, an ectonucleotide pyrophosphatase/phosphodiesterase involved in tissue calcification. Structure, 20(11), 1948–1959. 10.1016/j.str.2012.09.001 [PubMed: 23041369]

Kingman J, Uitto J, & Li Q (2017). Elevated dietary magnesium during pregnancy and postnatal life prevents ectopic mineralization in Enpp1asj mice, a model for generalized arterial calcification of infancy. Oncotarget, 8(24), 38152–38160. 10.18632/oncotarget.16687 [PubMed: 28402956]

Levy-Litan V, Hershkovitz E, Avizov L, Leventhal N, Bercovich D, Chalifa-Caspi V, … Parvari R (2010). Autosomal-recessive hypophosphatemic rickets is associated with an inactivation mutation in the ENPP1 gene. American Journal of Human Genetics, 86(2), 273–278. 10.1016/j.ajhg. 2010.01.010 [PubMed: 20137772]

Li Q, Kingman J, Sundberg JP, Levine MA, & Uitto J (2016). Dual effects of bisphosphonates on ectopic skin and vascular soft tissue mineralization versus bone microarchitecture in a mouse model of generalized arterial calcification of infancy. The Journal of Investigative Dermatology, 136(1), 275–283. 10.1038/JID.2015.377 [PubMed: 26763447]

Li Q, van de Wetering K, & Uitto J (2019). Pseudoxanthoma elasticum as a paradigm of heritable ectopic mineralization disorders: Pathomechanisms and treatment development. The American Journal of Pathology, 189 (2), 216–225. 10.1016/j.ajpath.2018.09.014 [PubMed: 30414410]

Lorenz-Depiereux B, Schnabel D, Tiosano D, Hausler G, & Strom TM (2010). Loss-of-function ENPP1 mutations cause both generalized arterial calcification of infancy and autosomal-recessive hypophosphatemic rickets. American Journal of Human Genetics, 86(2), 267–272. 10.1016/j.ajhg. 2010.01.006 [PubMed: 20137773]

Meradji M, de Villeneuve VH, Huber J, de Bruijn WC, & Pearse RG (1978). Idiopathic infantile arterial calcification in siblings: Radiologic diagnosis and successful treatment. The Journal of Pediatrics, 92(3), 401–405. [PubMed: 416189]

Meyre D, Bouatia-Naji N, Tounian A, Samson C, Lecoeur C, Vatin V, … Froguel P (2005). Variants of ENPP1 are associated with childhood and adult obesity and increase the risk of glucose intolerance and type 2 diabetes. Nature Genetics, 37(8), 863–867. 10.1038/ng1604 [PubMed: 16025115]

Nael A, Siaghani PJ, Chen D, Romansky SG, & Shane L (2014). Idiopathic infantile arterial calcification: A possible cause of refractory cardiopulmonary failure in infancy. Case Reports in Pathology, 2014, 189850 10.1155/2014/189850 [PubMed: 24660083]

Nitschke Y, Baujat G, Botschen U, Wittkampf T, du Moulin M, Stella J, … Rutsch F (2012). Generalized arterial calcification of infancy and pseudoxanthoma elasticum can be caused by mutations in either ENPP1 or ABCC6. American Journal of Human Genetics, 90(1), 25–39. 10.1016/j.ajhg.2011.11.020 [PubMed: 22209248]

Nitschke Y, & Rutsch F (2012). Generalized arterial calcification of infancy and pseudoxanthoma elasticum: Two sides of the same coin. Frontiers in Genetics, 3, 302 10.3389/fgene.2012.00302 [PubMed: 23269929]

Prior JT, & Bergstrom VW (1948). Generalized arterial calcification in infants. American Journal of Diseases of Children, 76(1), 91–101. [PubMed: 18117552]

Rutsch F, Boyer P, Nitschke Y, Ruf N, Lorenz-Depierieux B, Wittkampf T, … Group GS (2008). Hypophosphatemia, hyperphosphaturia, and bisphosphonate treatment are associated with survival beyond infancy in generalized arterial calcification of infancy. Circulation Cardiovascular Genetics, 1(2), 133–140. 10.1161/CIRCGENETICS.108.797704 [PubMed: 20016754]

Rutsch F, Nitschke Y, & Terkeltaub R (2011). Genetics in arterial calcification: Pieces of a puzzle and cogs in a wheel. Circulation Research, 109(5), 578–592. 10.1161/CIRCRESAHA.111.247965 [PubMed: 21852556]

Rutsch F, Ruf N, Vaingankar S, Toliat MR, Suk A, Hohne W, … Nurnberg P (2003). Mutations in ENPP1 are associated with 'idiopathic' infantile arterial calcification. Nature Genetics, 34(4), 379–381. 10.1038/ng1221 [PubMed: 12881724]

Thomas P, Chandra M, Kahn E, McVicar M, Naidich J, & LaCorte M (1990). Idiopathic arterial calcification of infancy: A case with prolonged survival. Pediatric Nephrology, 4(3), 233–235. [PubMed: 2400650]

van der Sluis IM, Boot AM, Vernooij M, Meradji M, & Kroon AA (2006). Idiopathic infantile arterial calcification: Clinical presentation, therapy and long-term follow-up. European Journal of Pediatrics, 165 (9), 590–593. 10.1007/s00431-006-0146-8 [PubMed: 16649023]

Van Dyck M, Proesmans W, Van Hollebeke E, Marchal G, & Moerman P (1989). Idiopathic infantile arterial calcification with cardiac, renal and central nervous system involvement. European Journal of Pediatrics, 148(4), 374–377. [PubMed: 2707283]

Vivante A, Hwang DY, Kohl S, Chen J, Shril S, Schulz J, … Hildebrandt F (2017). Exome sequencing discerns syndromes in patients from consanguineous families with congenital anomalies of the

kidneys and urinary tract. Journal of the American Society of Nephrology, 28(1), 69–75. 10.1681/ ASN.2015080962 [PubMed: 27151922]
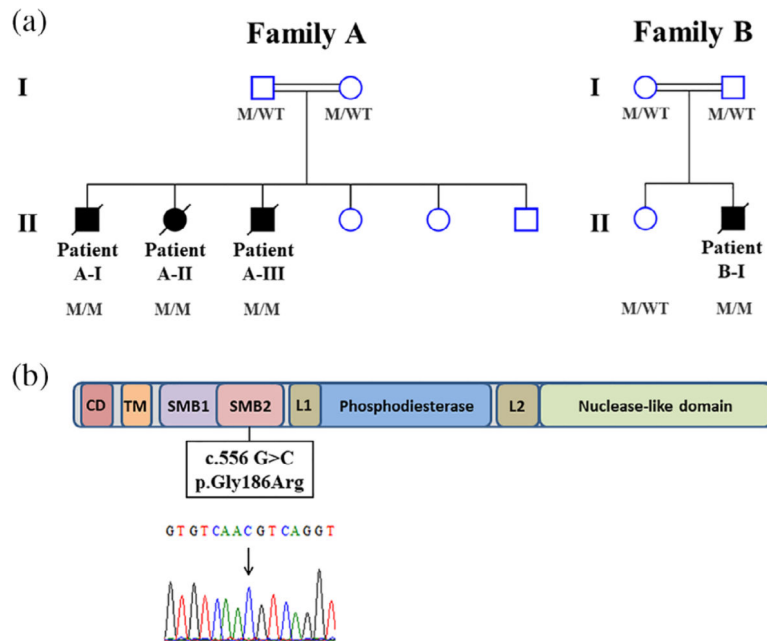
FIGURE 1.
Pedigree structures of Family A and Family B and the localization of the c.556G>C mutation in the somatomedin B domain. (a) The pedigree of Family A and Family B shows three and one affected members, respectively. Squares indicate male family members and circles female family members; filled squares and circles indicate affected individuals. Double lines between parents indicate that the parents are related. (b) Domain organization of human ENPP1 protein with the localization of the c.556G>C mutation in the highly conserved protein domain SMB2. Sanger sequencing chromatogram of the homozygous mutation, c.556G>C, in the *ENPP1* gene revealed by mutation analysis (arrow). M, mutation; SMB2, somatomedin B2; W, wild type [Color figure can be viewed at wileyonlinelibrary.com]
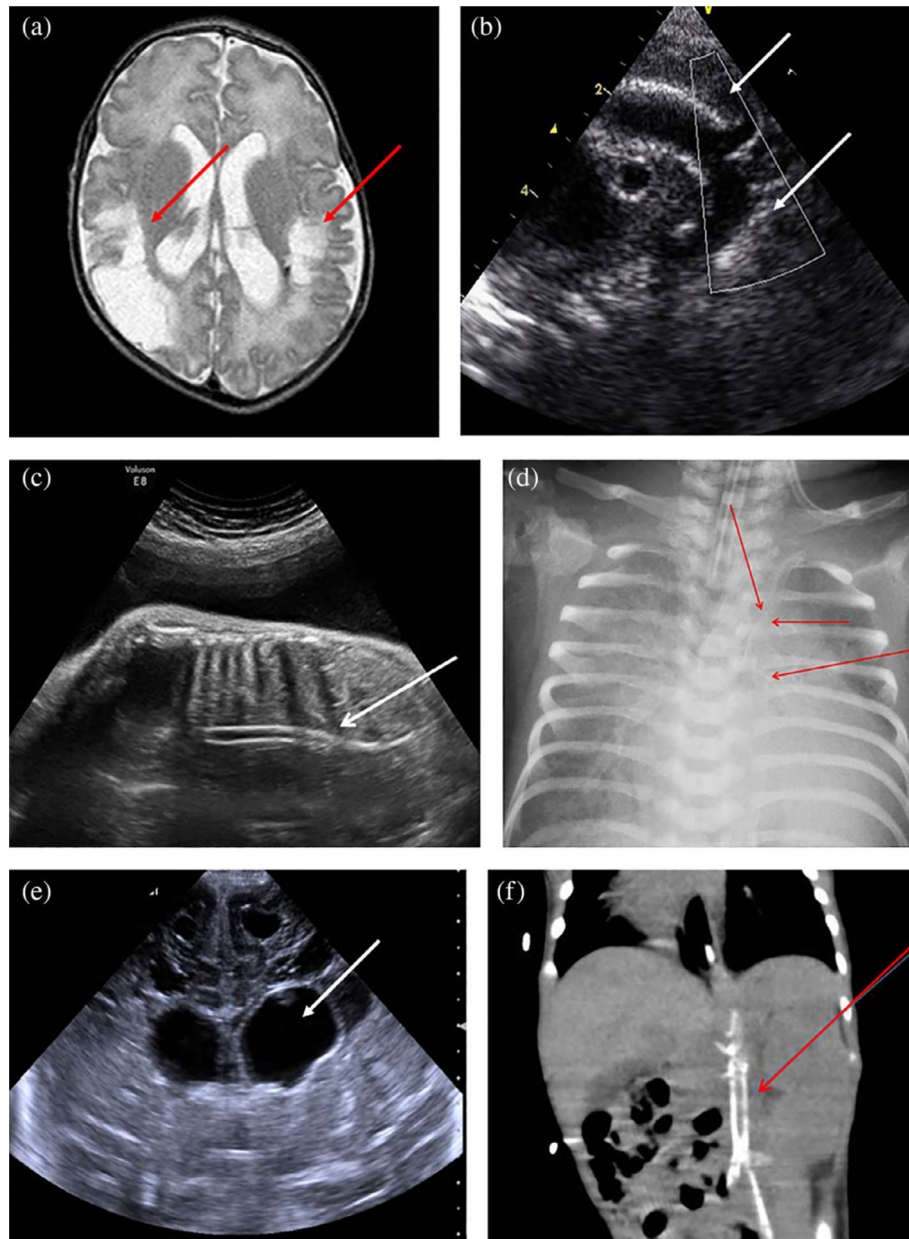
FIGURE 2.

Clinical and imaging findings in four affected patients. (a) Brain MRI of Patient A-I revealed bilateral ventriculomegaly with extensive parietooccipital gliosis (red arrows). (b) Echocardiography of Patient A-II demonstrated significant aortic calcifications (white arrows). (c, d) Substantial arterial calcifications demonstrated in Patient A-III were revealed by prenatal US (white arrow) (c) as well as in chest X-ray performed several days postdelivery (red arrows) (d). (e, f) Imaging analysis of Patient B-I; brain US revealed bilateral ventriculomegaly (white arrow) (e); abdominal CT scan revealed significant aortic and iliac artery calcifications (red arrow) (f). CT, computed tomography; MRI, magnetic resonance imaging; US, ultrasound [Color figure can be viewed at wileyonlinelibrary.com]

TABLE 1

Clinical phenotypes of affected individuals with ENPP1 mutations

	Patient A-I	Patient A-II	Patient A-III	Patient B-I
Gestational age (weeks)	33	33 + 5	33 + 1	36 + 2
CNS involvement	Old strokes, massive gliotic changes, and bilateral occipital necrosis	Left choroid plexus cyst with bilateral ventriculomegaly, and periventricular calcifications	Mild ventriculomegaly with lenticulostriate vasculopathy	Signs of global brain ischemia, cystic PVL, and later hydrocephalus
Hematological involvement	Thrombocytopenia polycythemia	Thrombocytopenia abnormal clotting	Thrombcytopenia	Thrombocytopenia
Endocrinological manifestations	Hypoglycemia	None	None	Hypoglycemia
Cardiovascular defects	Significant septal hypertrophy, mitral regurgitation, tricuspid regurgitation, and decreased contractility	Patent foramen ovale, patent ductus arteriosus, mild mitral regurgitation, and hypertrophy with pericardial effusion	Decreased contractility and hyper echogenicity of large blood vessels	Hypertrophy of left chamber secondary to systemic hypertension
Lung involvement	Respiratory distress	Respiratory distress	Respiratory distress	None
Hepatic involvement	Canalicular cholestasis with elevated liver enzymes	Mild hepatomegaly and ascites, with elevated liver enzymes	Elevated GGT	Elevated GGT
Age at death	2 months	3 days	11 days	6 months

Abbreviations: CNS, central nervous system; GGT, gamma-glutamyl transpeptidase; PVL, periventricular leukodystrophy.